Cancer Immunology, Immunotherapy (2025) 74:153
https://doi.org/10.1007/s00262-025-03995-4

RESEARCH

A novel peptide targeting CCR7 inhibits tumor cell lymph node metastasis

Yixuan Sun[1] · Yuzhen Qian[2] · Lu Qiu[1] · Xueqin Zhu[1] · Haoming Ning[1] · Liwei Pang[2] · Xiaoshuang Niu[1] · Yi Liu[1] · Xiuman Zhou[1] · Guanyu Chen[1] · Wenjie Zhai[2] · Yanfeng Gao[1]

Received: 27 August 2024 / Accepted: 21 February 2025 / Published online: 19 March 2025

Abstract

Lymph nodes are the most common metastasis sites for tumor cells, which are intimately linked to patient prognosis. It has been reported that cancer cells can upregulate CC Chemokine Receptor 7 (CCR7) expression and hijack its normal functions, enabling them to migrate along the gradient of CCL19 and CCL21 toward the lymph nodes and colonies as the initial stage of distant metastasis. In tumor patients, the metastatic tumor in the lymph nodes exhibited higher expression of CCR7, as well as inhibitory immune checkpoints PD-1, LAG-3, and TIM-3 compared to the primary tumors with the analysis of TCGA and GEO databases. Also, in mouse tumor model, tumor cells with elevated CCR7 expression were more susceptible to develop popliteal lymph node metastasis. Subsequently, we successfully identified a CCR7 binding peptide TC6 by phage display biopanning, which specifically blocks the interaction of CCR7/CCL19 and CCR7/CCL21. Further, the D-amino acids were introduced to substitute the N- and C-terminus of TC6 peptide to obtain the proteolysis-resistant TC6-D3 peptide, which decreased tumor cell migration in vitro via ERK1/2 pathway and inhibited tumor growth and lymph nodes metastasis in vivo, as well as effectively restored T cells cytotoxicity in both primary tumors and lymph nodes. In conclusion, CCR7 promoted tumor cell metastasis to lymph node and inhibited the anti-tumor immune responses in lymph nodes. Specific blockade of the CCR7 pathway with TC6-D3 peptide can significantly reduce lymph node tumor burden, promoting $CD8^+$ T cell infiltration in primary tumors, meanwhile, enhancing anti-tumor immune responses in lymph nodes.

Keywords CCR7 · Lymph node metastasis · Peptide · Blockade · Immune responses

Introduction

Lymph node (LN) metastasis represents a common feature across a wide range of solid tissue malignancies and closely associated with poor survival [1–3]. Cancer cells are often prior to regionally metastasize to adjacent LN before metastasizing systemically through the lymphatics and blood, which induces tumor-specific immune tolerance and thus renders distant tissues amenable to metastatic colonization [4]. Recent studies have revealed the decreased oxidative stress and ferroptosis in lymph, including higher levels of glutathione and oleic acid, lesser free iron in LN-protected melanoma cells from ferroptosis and increased their capacity to form metastatic tumors [5, 6]. Engleman et al. previously found that metastatic tumor cells in LN initially upregulated MHC-I and PD-L1 to evade cytotoxicity of natural killing (NK) cells and T cells in response to chronic interferon (IFN) signaling, altering the immune compartment within LN to induce antigen-specific Treg differentiation and immune tolerance, further promoting metastasis to distant tissues [4]. These findings indicate that tumor cells alter the metabolic pathways and phenotypes to escape immune surveillance in LNs. In addition, the specifically expressed chemokines in LNs induced the prior metastasis of tumor cells [7]. Since the chemokine receptors regulate immune cell migration and survival, that often stimulated by inflammatory signals, their expression on tumor cells may reflect

Yixuan Sun and Yuzhen Qian have contributed equally to this work.

✉ Wenjie Zhai
wjzhai@zzu.edu.cn

✉ Yanfeng Gao
gaoyf29@mail.sysu.edu.cn

[1] School of Pharmaceutical Sciences (Shenzhen), Sun Yat-sen University, Shenzhen 518107, China

[2] School of Life Sciences, Zhengzhou University, Zhengzhou 450001, China

aberrant inflammatory signals and lead to enhanced tumor growth, invasion, and metastasis.

Chemokines are a family of cytokines that mediate leukocyte trafficking. Among them, chemokine receptor 7 (CCR7) with C–C chemokine ligand 19/21 pair (CCL19/CCL21), which belong to the highly druggable G-protein-coupled receptor (GPCR) family, plays a vital role in the migration of dendritic cells (DCs) to LNs [8]. Since overexpressed CCR7 dramatically correlates with larger primary tumors, deeper lymphatic invasion, and poorer survival rates, CCR7 has emerged as an important biomarker for predicting the axillary LNs metastasis in melanoma [9], colorectal [10], breast [11], and esophageal squamous cell carcinoma [12], etc. Recently, it has been reported that cancer cells could upregulate CCR7 expression and hijacked its normal functions, enabling them to migrate along the gradient of CCL19 and CCL21 secreted by the lymphatic endothelial cells and high endothelial venules and toward the LN to colonize them as the first step toward metastasis [13] such as B16-F10, 4T1, and MCF7 mouse model [14–16]. In vivo studies revealed that the tumor growth, angiogenesis, and metastatic formation are decreased when downregulating CCR7 or applying CCR7 antagonists [15, 17]. Therefore, CCR7 is suggested as a promising therapeutic target and blocking the CCR7-CCL21/CCL19 axis can effectively inhibit the tumor growth and occurrence of LN metastasis.

Due to the central role of CCR7 in tumor metastasis, several therapeutic strategies have been developed to exploit this axis for cancer treatment, including siRNA interfering the CCR7 expression, antibodies, or small molecule inhibitors against CCR7. Recently, Joerg Standfuss et al. screened the small molecule inhibitor Cmp2105, specifically binding to the intracellular domain of CCR7 and inhibiting its activation [18], but its biological activity and the effects on inhibiting tumor cell metastasis to LNs in vivo remain obscure. In addition, Leaf Huang et al. delivered a plasmid encoding an antagonistic CCR7 protein trap by tumor-targeting nanoparticles in a highly metastatic 4T1 mouse model, which locally disrupted the CCR7 signaling pathways in the tumor site and efficiently inhibited 4T1 lymphatic metastasis [19]. Besides, it has been reported that CCR7 therapeutic antibody can effectively block the invasion and metastasis of tumor cells. Carlos Cuesta-Mateos et al. generated CAP-100, an antibody specifically binds to human CCR7 and neutralizes its ligand binding site and intracellular signaling pathways, as well as strongly inhibits the CCR7-induced migration, extravasation, homing, and survival in CLL samples in vitro and in vivo preclinical models, and the clinical trial (NCT04704323) to evaluate this novel therapeutic approach in CLL patients is pending [20]. Accordingly, all results validated that targeting CCR7 is an effective therapeutic strategy to prevent the access of tumor cells into the LN niches, which has a vital clinical application value.

Peptides have excellent biological activity, including lesser treatment-related adverse events, better tumor penetration, and easier synthesis and modification with lower cost, as compared to therapeutic antibodies [21–23]. Currently, several peptides targeting G-protein-coupled receptors (GPCR) have recently entered the clinical trials and pharmaceutical markets [24]. In particular, Mavorixafor, an antagonistic peptide targeting CXCR4, has demonstrated potential anti-tumor activity and a manageable safety profile in pancreatic ductal adenocarcinoma [25], relapsed/refractory acute myelogenous leukemia [26], and advanced renal cell carcinoma [27] with decreased immunosuppressive cells as well as increased activated cytotoxic T cell infiltration in tumor microenvironment in clinical trials. However, there are no peptide inhibitors reported to specifically block the CCR7 axis. Therefore, to develop the peptides blocking the CCR7 axis to explore the potential application was absolutely crucial for restraining LNs metastasis.

Here, we successfully identified a CCR7 binding peptide TC6 by phage display, and D-amino acids were introduced to substitute the N- and C-terminus of TC6 to generate the hydrolysis-resistant peptide TC6-D3, which was able to specifically block the interaction of CCR7/CCL19 and CCR7/CCL21 and effectively inhibited the migration of tumor cells via ERK1/2 signal pathway in vitro. Additionally, TC6-D3 decreased the LNs metastasis of MC38 tumor cells in an in vivo popliteal LN metastasis model. Our study firstly proposed a novel strategy to amplify anti-tumor immune response and reduce LN tumor burden as well.

Materials and methods

Cell lines

B16 and CHO-K1 cell lines were cultured with complete RPMI 1640 medium containing 10% heat-inactivated fetal bovine serum (FBS, Gibco), 100 U/mL penicillin, and 100 mg/mL streptomycin (Solarbio, China). MC38 cell line was cultured with complete DMEM. B16-CCR7 cell line was gifted by Professor XM Yang from the School of Life Science and Technology, Shanghai Jiao Tong University. MC38-CCR7 (GFP) cell line was established by lentiviral transfection. All cell lines were cultured in an incubator at 37 °C with 5% CO_2 incubator.

Plasmid construction and transfection

Mouse CCR7 cDNA was cloned into the pLVX-IRES-ZsGreen1 plasmid at first. A lentivirus transfection system was used to establish the stable CCR7 overexpression MC38 cells. Besides, the CCR7 cDNA without the stop codon was cloned into the pLVX-puro EGFP plasmid to obtain

CCR7-EGFP fusion protein. The CHOK1-CCR7-EGFP cells with intensely green fluorescence were established by transient transfection with the plasmid and used for microscale thermophoresis (MST) assay. The culture conditions of the cells were consistent with CHOK1 cells.

Phage-displayed peptide screening for CCR7

Ph.D.-12 peptide library (New England BioLabs, Beijing, China) was used for peptide screening. The screening process is based on previous report [28]. Briefly, B16 and B16-CCR7 cells (1×10^6 cells) were harvested and washed with serum-free medium and blocked with 0.5% bovine serum albumin at 4 °C for 1 h. Then, B16 cells were incubated with Ph.D.-12 peptide library (2×10^{11} phages) for 2 h at 4 °C, and the supernatant containing unbound phages was incubated with B16-CCR7 cells (1×10^6 cells) for 2 h at 4 °C. After washing with PBST (0.1% Tween-20) for 8 times, the phages were eluted with 200 mM glycine–HCl (pH 2.2) for 20 min and neutralized with 1 M Tris–HCl (pH 9.1). Then, we utilized *E. coli* (ER2738) as the host for the amplification of the binding phages. The phage screening process was repeated five times. The sequences of phages were determined by DNA sequencing.

Blocking assays

Based on the sequencing results, candidate peptides targeted CCR7 were synthesized using solid-phase peptide synthesis. For blocking the interaction of CCR7/CCL19 or CCR7/CCL21, candidate peptides were incubated with B16-CCR7 cells at 4 °C for 30 min. Subsequently, recombinant CCL19-His (50047-M08B, Sino Biological) or CCL21-His protein (58025-M08B, Sino Biological) was added into the mixture for 30 min and further incubated with anti-His-APC (BioLegend, 362605) antibody for 30 min in turn. The system without peptides was used as positive control (P). The cells were only incubated with the anti-His-APC antibody served as a negative control (N). The mean fluorescence intensity (MFI) was tested by Flow cytometry (BD Fortessa). The blocking rate was calculated by the formula: blocking rate (%) = (MFI of P-MFI of tested peptides)/(MFI of P-MFI of N) × 100%.

Molecular docking

Molecular docking was performed using the Molecular Operating Environment software (MOE, Version: 2020, Chemical Computing Group ULC, Canada). Firstly, the crystal structure of human CCR7 (PDB ID: 6QZH) was downloaded from the RCSB Protein Data Bank (PDB) (https://www1.rcsb.org/). The crystal structure of mouse CCR7 was obtained by homology modeling using the structure of human CCR7 as a template within the MOE software. Subsequently, the structure of TC6 peptides was predicted by the online tool PEPstrMOD (https://webs.iiitd.edu.in/raghava/pepstrmod/). Both the protein and peptide performed energy minimization before molecular docking. The active pocket and binding area of mouse CCR7 were flexibly docked with TC6 peptides (parameter: induced fit) by MOE software. Finally, according to the overall score (S value) and better docking pose, an optimal peptide–protein interaction model was chosen.

MST

The affinity of candidate peptides to CCR7 was tested by microscale thermophoresis (MST) (NanoTemper Technologies GmbH, Germany). Firstly, CHOK1-EGFP and CHOK1-mCCR7-EGFP cell membranes were extracted with the cell membrane extraction kit (P1201, APPLYGEN). The extraction procedure was performed according to the instructions. Further, EGFP and CCR7-EGFP fusion protein was diluted into gradient concentrations with PBST (0.05% Tween-20) for 16 times and then loaded into capillary for fluorescence analysis, and the concentration of the protein with the capillary exhibiting fluorescence intensity around 400 is selected for the following test. Analogously, TC6-D3 peptide was diluted into gradient concentrations and then mixed with the equal volumes of cell membrane proteins solution at room temperature for 5 min following the MST assay. Then, the mixture was loaded into the capillary for further detection of the dissociation constant (K_D) values, which were calculated by the Nano Temper analysis software MO. Affinity Analysis.

The stability of peptides detected by RP-HPLC

TC6 and TC6-D3 peptides were dissolved in normal saline and diluted with 10% mouse serum to the concentration of 0.2 mM and incubated at 37 °C incubator for 0.25 h, 0.5 h, 1 h, 2 h, 4 h, 8 h, 16 h, 24 h, and 48 h, respectively. Then, 200 µL samples were taken at each time point and immediately mixed with 100 µL of 10% $HClO_4$ solution followed by centrifugation at 12,000 rpm for 10 min twice. Analytical RP-HPLC (Waters 2695, Waters, USA) was performed to determine the residual of the peptides.

MTT assay

The effects of TC6-D3 peptide on the proliferation of MC38-CCR7 (GFP) cell lines were determined by MTT assay. Briefly, cells were seeded into 96-well culture plates at the density of 4000 cells/well and incubated with gradient concentrations TC6-D3 peptide at 37 °C incubator for 24 h, 48 h, and 72 h, respectively. The cell viability was measured

at each time point using 5 mg/mL MTT reagent (Sigma, M2003) dissolved in PBS and incubated at 37℃ for 4 h. After removing the incubation medium, formazan crystals were dissolved in 150 µL DMSO. Absorbance was monitored by a microplate reader (SpectraMax iD5) at 490 nm wavelength.

Western blot

The effects of TC6-D3 peptide on the phosphorylation of ERK1/2 in tumor cells were determined by Western blot. Before the addition of CCL19 (250-27B, PeproTech) or CCL21 (250–13, PeproTech), tumor cells were treated with peptide at the concentration of 200 µM. Cells were harvested and washed twice with PBS. After centrifugation at 12,000 rpm for 10 min. The concentration was determined by a BCA protein assay kit (C503061, Sangon Biotech). The protein was boiled with loading buffer for 10 min and separated by SDS-PAGE. The protein was transferred to the PVDF membranes and blocked for 2 h by 5% defatted milk (pH7.2 TBS containing 0.1% Tween-20) at room temperature. The membranes were incubated with anti-ERK1/2 (9102, Cell Signaling Technology) and anti-pERK1/2 (9101, Cell Signaling Technology) at 4 °C overnight. The membranes were washed five times and incubated with HRP-conjugated Goat Anti-Rabbit IgG (D110058, Sangon Biotech) for 2 h. Blots were detected by ECL system (Azure C600, USA).

Chemotaxis assay

Cells chemotaxis assay was performed using the 24-well transwell system (8 µm aperture). MC38-CCR7 (GFP) and control cell lines MC38-V (GFP) (1×10^5 cells/well) resuspended in 200 µL complete DMEM were seeded in the upper chambers with or without 200 µM of TC6-D3 peptide, and 600 µL complete DMEM with 100 ng/mL of CCL19 was added to the lower chambers for 48 h. The cells in upper chambers were erased with cotton swabs and washed twice with PBS. The migrated cells were fixed with 4% paraformaldehyde for 30 min and stained with 0.2% crystal violet for 30 min. The migration of cells was recorded by an inverted microscope and quantified with the ImageJ software.

Mouse popliteal lymph node metastasis model

Female C57BL/6 mice (6 to 8 week old) were purchased from the Zhuhai BesTest Bio-Tech Co., Ltd. (Zhuhai, China) and raised under SPF conditions. The footpad tumor model was established as described previously [14, 29]. Briefly, 1×10^6 MC38-CCR7 (GFP) or MC38-V (GFP) cells were resuspended in 20 µL PBS and subcutaneously injected into the right footpad of mice. TC6-D3 peptide with a dosage of 2 or 6 mg/kg was administered every day when the tumor volume reaches about 150 mm^3 with the normal saline as negative control. Tumor volumes and body weight were measured every three days during the treatment for 14 days. The tumor cells metastasized to LN were detected through IVIS Lumina III and Flow cytometry. All animal experiments were approved by the Ethics Committee of School of Pharmaceutical Sciences (Shenzhen), Sun Yat-sen University (Approval No. SYSU-YXYSZ20230324).

Flow cytometry

Tumors were dissected from the footpad and finely chopped with scissors. The single-cell suspensions were prepared with collagenase IV (100 U/mL, 17104019, Gibco) and DNAse I (100 U/mL, DN25, Sigma) at 37℃ for 1 h. Also, lymph nodes were dissociated mechanically into single-cell suspensions to conduct intracellular cytokine staining assay. The immune cells were stimulated with 20 ng/mL PMA (P8139, Sigma, USA), 1 µM ionomycin (407952, Sigma, USA) and seeded in 24-well plates at the density of 2×10^6 cells/well in the presence of Golgiplug protein transport inhibitor (555029, BD Pharmingen, USA) for 4 h at 37℃. The secretion of IFN-γ from $CD8^+$ T cells was analyzed by flow cytometry. For monocytes staining, cells were blocked with 10% rat serum for 15 min and incubated with antibodies for 30 min at 4 °C.

All antibodies used for flow cytometry as below: Anti-mouse CD45-PE (103105), and anti-mouse CCR7-BV605 (120125) were purchased from BioLegend. Anti-mouse CD45-FITC (11-0451-85), anti-mouse CD3-PerCP-eFluor710 (46-0032-82), anti-mouse CD8α-APC (17-0081-83), anti-mouse CD8α-PE (12-0081-85), anti-mouse CD11c PE-Cyanine7 (25-0114-81), anti-mouse CD11b-eFlour450 (48-0112-82) and anti-mouse IFN-γ-APC (17-7311-82) were purchased from eBioscience. Cells were tested by Flow cytometry (BD Fortessa) and analyzed with FlowJo software.

Statistical analysis

Data were analyzed using GraphPad Prism (Version 8.0), and results were expressed as the mean ± standard error of the mean from three independent experiments. Statistical differences between two groups were evaluated with one-tailed unpaired Student's *t* test. Values of $P < 0.05$ were considered to be significant difference. $^*P < 0.05$, $^{**}P < 0.01$, and $^{***}P < 0.001$.

Results

The expression of CCR7 correlated with the LN metastasis

Metastasis is the primary cause of death in cancer patients, and LN is the highest risk of being invaded by malignant cells. The dependency of tumor cells on CCR7 for LN metastasis has been demonstrated in previous studies, while the impact of tumor cells to LN on anti-tumor immune response needs further exploration. To investigate the essential role of CCR7 in tumor metastasis, we analyzed CCR7 expression by GEO and TCGA datasets. The results showed that CCR7 was highly expressed in tumors with LN metastasis, while expressed in a lower level in primary tumors. This phenomenon was observed in a variety of solid tumors, including colorectal cancer (CRC), breast cancer (BC), oral squamous cell carcinoma (OSCC), and melanoma (Fig. 1A–E). This phenomenon is consistent with the previous reports that CCR7 axis plays a critical role in regulating the migration of tumor cells toward the lymphatic system and facilitating metastasis [13]. Additionally, the expression level of CCR7

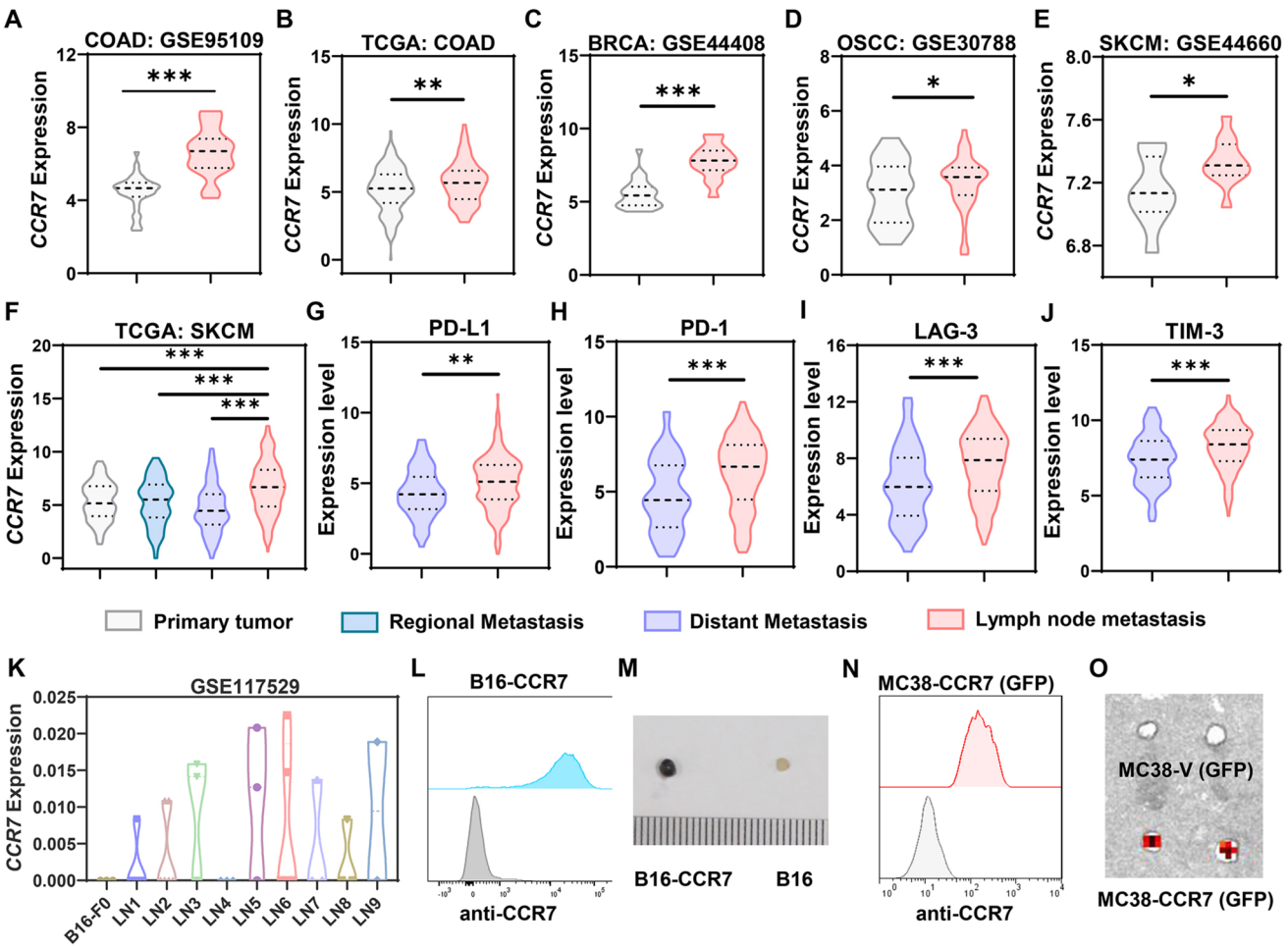

Fig. 1 The expression of CCR7 correlated with the LN metastasis. **A–E** The expression of CCR7 in primary tumor and lymph node metastasis tumor tissue among multifarious cancer types analyzed by GEO datasets (GSE95019, GSE44408, GSE30788, and GSE44660) and TCGA datasets. **F** The expression of CCR7 in primary tumor, regional metastasis, distant metastasis, and lymph node metastasis tissue in skin cutaneous melanoma (SKCM) analyzed by TCGA dataset. **G–J** The level of PD-L1, PD-1, LAG-3, and TIM-3 in distant metastasis and lymph node metastasis tissue of SKCM. **K** The expression level of CCR7 in LN metastatic tumor lines developed by serial in vivo lymph node metastases selection in the GSE117529 dataset. **L** The expression of CCR7 in B16-CCR7 cell line tested by Flow cytometer. **M** The effect of B16-CCR7 and B16 cell lines metastasized to adjacent popliteal lymph node after being injected into mouse footpad for 22 days. The popliteal lymph nodes were surgically excised and photographed. **N** The expression of CCR7 in the MC38-CCR7 (GFP) cell line tested by Flow cytometer. **O** The effect of MC38-CCR7 (GFP) and MC38-V (GFP) cell lines metastasized to adjacent popliteal lymph node after injected into mouse footpad for 22 days. The popliteal lymph nodes were surgically excised and detected with IVIS imaging. Statistical significance was determined by unpaired Student's *t* test. $^{*}P<0.05$, $^{**}P<0.01$, $^{***}P<0.001$

within skin cutaneous melanoma (SKCM) among primary tumor, regional metastasis, and distant metastasis tissue were comparable, while the tumor cells with LN metastasis exhibited the highest level of CCR7 by analyzing the TCGA datasets (Fig. 1F). Further, compared with the tumors of distant metastasis, the negative immune checkpoint, including PD-L1, PD-1, LAG3, and remarkably TIM-3, was significantly elevated in LN metastasis tissue (Fig. 1G–J). These findings indicated that CCR7 not only mediated the tumor lymphatic metastasis but also facilitated the immunosuppressive microenvironment by notably unregulated exhausted makers to inhibit the activation of $CD8^+$ T cells, which further advanced the LN colonization and induced tumor immune tolerance to promote distant metastasis.

E.G. Engleman et al. developed a model of LN metastasis through serial in vivo selection to generate LN metastatic tumor cell lines named LN1 to LN9 that all metastasized to LNs at a higher frequency than the parental B16-F0 cell and exhibited variable transcriptional and epigenetic profiles to facilitate tumor evading the monitor of NK and T cells [4]. Here, we found LN metastatic tumor cell lines LN1 to LN9 exhibited higher CCR7 expression compared to the parental B16-F0 cell by analysis of GSE117529 dataset (Fig. 1K). Furthermore, we assumed CCR7 plays a pivotal role in tumor metastasizing to LNs and constructed the B16-CCR7 and MC38-CCR7 (GFP) cell lines (Fig. 1L and N) to establish a popliteal LN metastasis model by transplanting the cells into the right footpad of mice. The role of CCR7 was validated in the model, which is consistent with the previous report that overexpressed CCR7 in MC38 and B16 cells augmented the LN metastasis (Fig. 1M and O). The results illustrated the potential value of targeting CCR7 pathway for relieving LN burden and enhancing cancer immunotherapy.

Screening of CCR7 peptide by phage display library

We performed phage display biopanning to screen peptides targeting CCR7 and designated six peptides named TC1 to TC6 after 5 rounds of subtractive biopanning using B16 and B16-CCR7 cells (Fig. 2A). Preliminary blocking assays were conducted to evaluate the blocking efficacy of candidate peptides, and TC6 (Figure S1) exhibited the strongest effect on the interference of both CCR7/CCL19 and CCR7/CCL21 interaction (Fig. 2B, C). TC6 peptide also displayed a dose-dependent effect on blocking CCR7/CCL19 and CCR7/CCL21 interaction with IC_{50} values of 175.8 ± 15.6 μM and 255.7 ± 36.7 μM, respectively (Fig. 2D, E). Alanine scanning was performed to determine the contribution of each residue of TC6 peptide to their blocking activities (Fig. 2F). As expected, each of mutants decreased the blocking efficacy of peptides on blocking CCR7/CCL19 interaction (Fig. 2G), particularly Leu1. Moreover, the spatial structure of TC6 peptide was predicted by online tool PEPstrMOD, and the crystal structure of mouse CCR7 was obtained by homology modeling using the structure of human CCR7 as a template within the MOE software (Figure S2). The TC6 peptide was docked to mCCR7 with MOE docking. By analysis of the docking results, the residues Asn4, Lys69, Asn151, Arg158, and Cys159 located in the pocket of CCR7 extracellular domain interacted with Leu1, Ser2, and Thr12 residues in TC6 peptide (Fig. 2H). Although other amino acids did not directly interact with CCR7, they contributed to maintaining the conformation of TC6 and facilitating its binding to CCR7. Additionally, considering the intrinsic conformational flexibility of the peptide, we predicted potential binding modes with the target protein, providing a structural framework for future functional optimization.

Enhancing the stability of TC6 peptide by D-amino acid substitution

The major limitations of L-peptide for application are its low stability caused by the degradation of proteases, and non-natural D-amino acids substitution strategy could solve this problem. Thus, the residues of TC6 peptide from both the N- and C-terminal were substituted by D-amino acids to improve the stability (Fig. 3A). The blocking assay showed that TC6-D3 retained the equivalent blocking activity toward CCR7/CCL19 interaction compared with TC6 peptide (Fig. 3B). Subsequently, RP-HPLC determined TC6 peptide quickly completely degraded within 24 h when incubated with 10% mouse serum, while TC6-D3 peptide showed potent hydrolysis resistance at 48 h (approximately 70%) (Fig. 3C–E). Next, we extracted the membrane protein of CHOK1-mCCR7-EGFP and CHOK1-EGFP cells to measure the specifical affinity of TC6-D3 to CCR7 using MST. The results showed the dissociation constant of TC6-D3 with mCCR7-EGFP fusion protein was 403 nM, but without interaction with the control EGFP protein with the $K_D > 1000$ μM (Fig. 3F, G). In addition, the role of TC6-D3 in cell proliferation was measured by MTT assay, and results revealed that TC6-D3 had no significant inhibitory effect on the proliferation of MC38-CCR7 (GFP) cells (Fig. 3H). Together, the peptide TC6-D3 with high binding affinity and blocking activity to the CCR7 pathway was developed, which showed superior biological stability and safety.

We predicted the structure of TC6-D3 and performed molecular docking studies between the TC6-D3 and the CCR7 receptor (Figure S3A). The results revealed conformational changes in the N-terminal region of TC6-D3 due to the D-amino acid substitution. Additionally, the residues L1, S2, D11, and T12 of TC6-D3 peptide interacted with the key amino acid residues S246, D155, and K69 on CCR7 receptor (Figure S3B). These structural changes were strongly

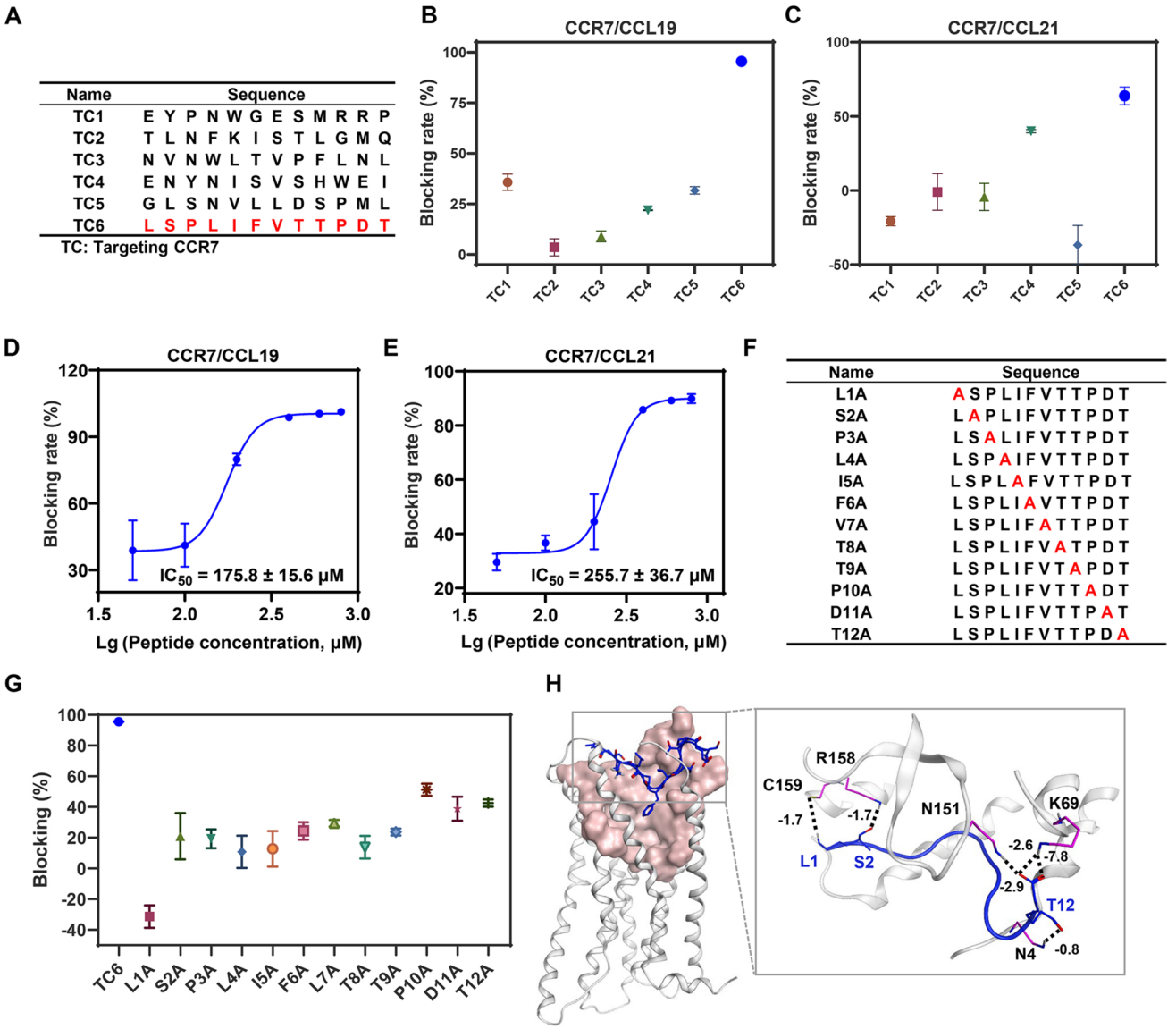

Fig. 2 Screening of CCR7 peptide by phage display library. **A** The sequences of candidate peptides targeting CCR7 screened by phage peptide library. **B**, **C** The blocking efficacy of candidate peptides on interfering CCR7/CCL19 (B) and CCR7/CCL21 (C) at the concentration of 200 μM ($n=3$). **D**, **E** Dose–response curves of TC6 on interfering CCR7/CCL19 (D) and CCR7/CCL21 (E) interaction ($n=3$). **F** The sequences of alanine scanning peptides. **G** The blocking efficacy of alanine scanning peptides on interfering CCR7/CCL19 interaction at the concentration of 200 μM ($n=3$). **H** Molecular docking was carried out in MOE software. The data are representative of at least three independent experiments and presented as mean ± SEM

correlated with the intrinsic conformational flexibility of the peptide and D-amino acid substitution.

TC6-D3 attenuated ERK1/2 phosphorylation

Strong evidence suggests that CCR7 engaged with CCL19 or CCL21 activates the ERK1/2 pathway to mediate the tumors migration and invasion [30, 31]. We examined whether TC6-D3 could affect the metastasis of MC38-CCR7 (GFP) cells and activation of intracellular signal. Primarily, transwell migration assays revealed that the chemokine CCL19 could significantly promote the migration of MC38-CCR7 (GFP) cells, while only a weak effect on the migration of control MC38-V (GFP) cells, indicating a CCL19/CCR7-dependent cell migration. TC6-D3 peptide significantly inhibited the migration of MC38-CCR7 (GFP) cells (Fig. 4A). Next, to investigate the inhibitory effect of TC6-D3 peptide on intracellular signals after blocking CCR7/CCL19 and CCR7/CCL21 interaction, Western blot assay verified that the phospho-ERK1/2 level was markedly increased in MC38-CCR7 (GFP) cells with the treatment of chemokines CCL19 or

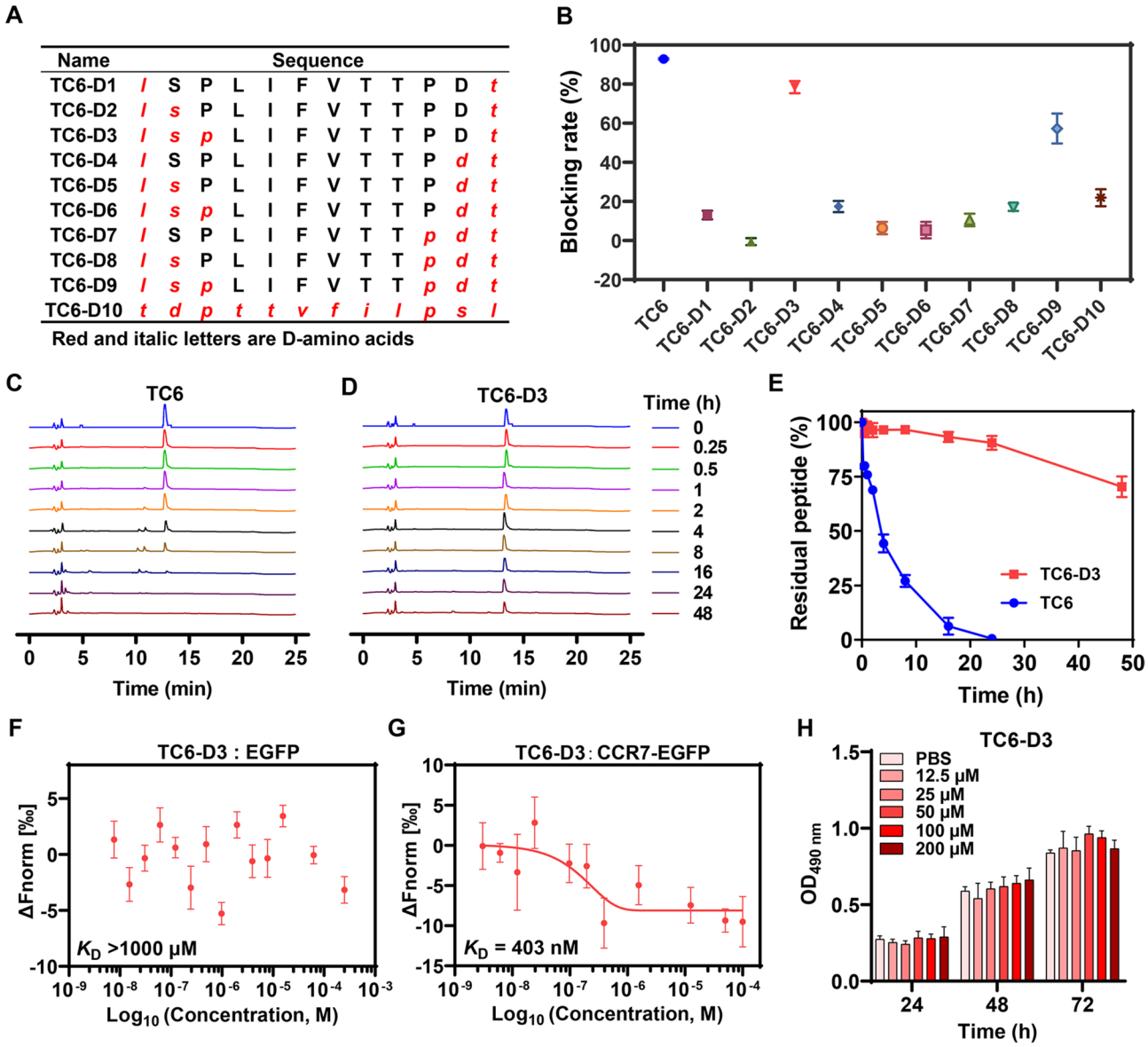

Fig. 3 Enhancing the stability of TC6 peptide by D-amino acid substitution. **A** The sequences of peptides substituted with D-amino acids from both N- and C- terminus of TC6. **B** The blocking efficacy of D-amino acid modified peptides on interfering CCR7-CCL19 interaction at the concentration of 200 μM ($n=3$). **C**–**E** RP-HPLC was utilized to detect the degradation of TC6 and TC6-D3 in 10% mouse serum ($n=3$). **F**, **G** The binding affinity of TC6-D3 peptide to CHOK1-CCR7-EGFP (F) and CHOK1-EGFP (G) cells membrane fusion protein was tested by MST ($n=3$). **H** The effect of TC6-D3 on the proliferation of MC3-CCR7 (GFP) tumor cell was determined by MTT assay ($n=3$). The data are representative of at least three independent experiments and presented as mean ± SEM

CCL21 within 5 min; the TC6-D3 peptide could significantly inhibit the phosphorylation (Fig. 4B, C). Besides that, the effects of peptide TC6-D3 on the phosphorylation of ERK1/2 in B16-CCR7 cells were consistent with that in MC38-CCR7 (GFP) cells (Fig. 4D, E). These results intensively suggested TC6-D3 peptide can attenuate the migration of tumor cells and inhibit the phosphorylation of ERK1/2 by specifically interfering in CCR7/CCL19 and CCR7/CCL21 interaction.

Sequence specificity of TC6-D3

To address the specificity of TC6-D3, we synthesized a scrambled-sequence control peptide (sequence: L*s*ITP*t*-DVT*lp*F) and confirmed its molecular weight using mass spectrometry (Figure S4). The MST assay revealed that the scrambled peptide exhibited no affinity to CCR7 protein (Figure S5A). Furthermore, in the blocking assays, the scrambled peptide showed no significant interference on

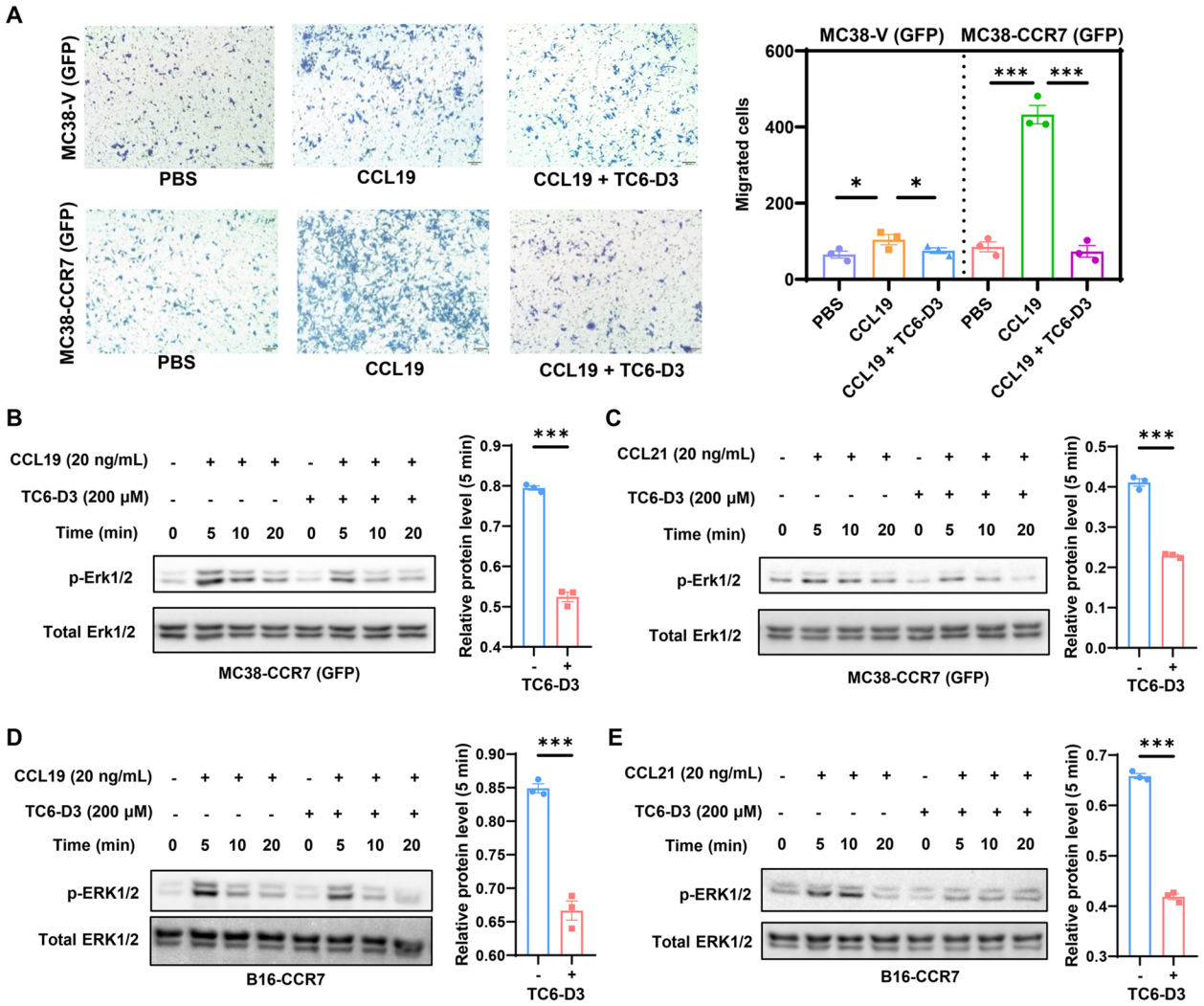

Fig. 4 TC6-D3-attenuated ERK1/2 phosphorylation. **A** Transwell assay was performed using MC38-V or MC38-CCR7 (GFP) cell lines with or without 200 μM TC6-D3 peptide when induced with 100 ng/mL chemokines CCL19 ($n=5$). **B**, **C** Western blot analysis of ERK1/2 phosphorylation in MC38-CCR7 (GFP) cells with or without 200 μM TC6-D3 peptide in the condition of 20 ng/mL chemokines CCL19 (B) or CCL21 (C) ($n=3$). **D**, **E** The same ERK1/2 phosphorylation in B16-CCR7 cells under the treatment of 20 ng/mL chemokines CCL19 (D) or CCL21 (E) ($n=3$). The data are presented as mean ± SEM. Student's *t* test, $^{*}P<0.05$, $^{**}P<0.01$, $^{***}P<0.001$

the binding of CCL19 to CCR7, whereas TC6-D3 peptide markedly inhibited this interaction (Figure S5B), as well as the scrambled peptide has no obvious effect on the chemotactic migration of MC38-CCR7 (GFP) cells in the transwell migration assays, in contrast to the significant inhibition observed with TC6-D3 (Figure S5C). This functional distinction was further supported by Western blot analysis, which demonstrated that the scrambled peptide did not significantly suppress ERK1/2 phosphorylation (Figure S5D), a key downstream indicator of CCR7 activation. Taken together, these results unequivocally demonstrate that the biological activity of TC6-D3 is sequence-specific and mediated through highly precise interactions with CCR7.

TC6-D3 reduced the LN tumor burden in popliteal LN metastasis model

The popliteal LN metastasis model was established by inoculating MC38-CCR7 (GFP) tumor cells on the footpad, in which the tumor cells could metastasize to the nearby popliteal LN and colonized to suppress the anti-tumor immunity and generate metastasis-promoting tumor-specific immune tolerance. The effects of TC6-D3 peptide on the tumor metastasis and anti-tumor immunity were explored. The schematic of peptide administration is shown in Fig. 5A. A dosage of 2 mg/kg or 6 mg/kg TC6-D3 peptide was intraperitoneally injected and normal saline as control group after tumor implantation for 9 days. Tumor growth curves showed

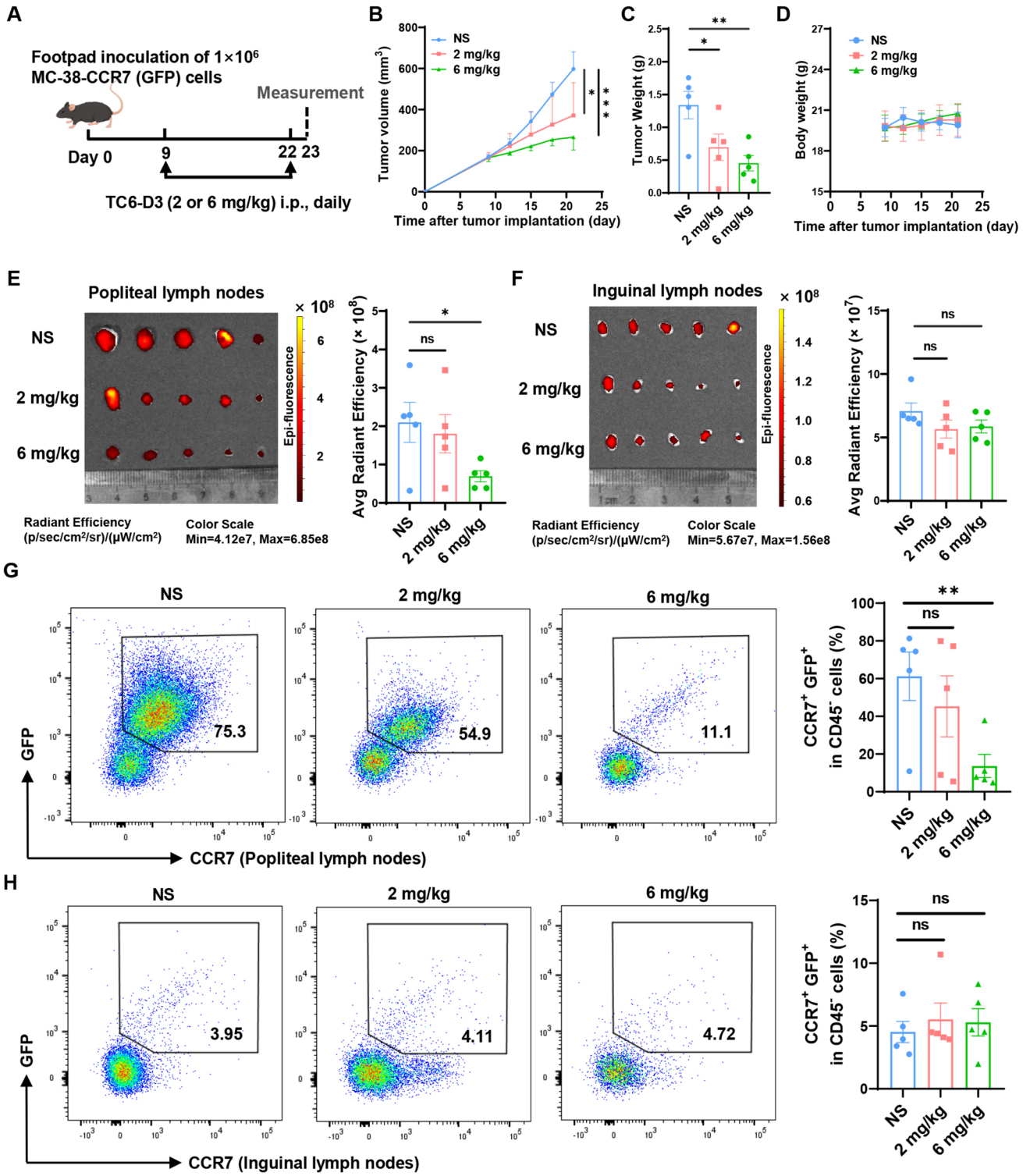

Fig. 5 TC6-D3 reduced the LN tumor burden in popliteal LN metastasis model. **A** Schematic of TC6-D3 peptide treatment on MC38-CCR7 (GFP) footpad tumor model. Mice were treated with TC6-D3 peptide intraperitoneally daily for 14 days. **B** Tumor growth curve of MC38-CCR7 (GFP) tumor-bearing mice treated with normal saline or TC6-D3 peptide ($n=5$). **C** Statistical analysis of tumor weight between different groups at the experimental endpoint ($n=5$). **D** TC6-D3 peptide did not affect the body weight after treatment for 14 days ($n=5$). **E**, **F** Tumor cells metastasized to popliteal (E) and inguinal (F) lymph nodes were detected with IVIS imaging ($n=5$). **G**, **H** The frequencies of $CCR7^+GFP^+$ tumor cells infiltrated in popliteal (G) and inguinal (H) lymph nodes were analyzed by flow cytometry ($n=5$). Data are represented as means ± SEM. Student's *t* test, $^*P<0.05$, $^{**}P<0.01$, $^{***}P<0.001$, ns, not significant

that TC6-D3 treatment slowed tumor growth at the 2 mg/kg dose, and the high dose group exhibited more eminent anti-tumor activity (Fig. 5B). The tumor weight showed the same trend (Fig. 5C), while the body weight of tumor-bearing mice followed TC6-D3 administration showed no significant change compared with the negative control (Fig. 5D). To analyze the effects of TC6-D3 peptide on LNs tumor burden following the completion of the treatment, we separated the LNs and conducted IVIS imaging to track tumor metastasis in vitro by tracking the green fluorescent within MC38-CCR7 (GFP) cells. TC6-D3 peptide demonstrated significant inhibition of popliteal LN metastasis (Fig. 5E) at a dose of 6 mg/kg but not inguinal LN (Fig. 5F). Similarly, we found the ratio of $CCR7^+GFP^+$ tumor cells in popliteal LN that were significantly reduced in TC6-D3 treated groups by flow cytometry (Fig. 5G), while tumor cells in inguinal LN showed no significant change (Fig. 5H). The phenomenon may be ascribed to the inclination of early-stage tumors that priorly metastasize toward the nearest LN. Overall, these results supported that TC6-D3 peptide suppressed the tumor LN metastasis through blocking CCR7 to interact with its ligands.

TC6-D3 restored T cell-mediated anti-tumor immunity

Here, we analyzed the correlation between the anti-tumor activity and the immunomodulatory effects of TC6-D3 peptide and found the ratio of tumor-infiltrating $CD8^+$ T cells (Fig. 6A) and cytotoxic IFN-γ-secreting $CD8^+$ T cells (Fig. 6B) in primary footpad tumor slightly increased in 2 mg/kg group, but intensively elevated in 6 mg/kg group. As previously mentioned, $CD8^+$ T cells in LN metastasis tissue highly expressed exhausted maker PD-1, LAG-3, and TIM-3. Therefore, we tested the percentages of IFN-γ-producing $CD8^+$ T cells and $CD4^+$ T cells in popliteal lymph node and inguinal lymph nodes by flow cytometry, as speculated that $CD8^+$ T cells secreting IFN-γ significantly increased in both popliteal (Fig. 6C) and inguinal lymph nodes (Fig. 6D) after treated with TC6-D3 peptide. In addition, we analyzed $CD8^+$ T cell infiltration and tumor apoptosis in primary tumor by immunofluorescence (Figure S6). These were the possibility that tumor cell apoptosis might be increased when plentiful $CD8^+$ T cell infiltrated into tumor tissue. This suggested that TC6-D3 peptide induced systemic immune response. All results indicated that CCR7 blocking peptide TC6-D3 inhibited LN metastasis to reduce tumor burden for restoring T cell anti-tumor response in LN.

TC6-D3 has no obvious immune-related side effects

Under steady-state or inflammatory conditions, CCR7-mediated signals controlled the migration of immune cells, especially DCs and T cells, homing to secondary lymphoid organs and subsequently positioning them within defined functional compartments, thus participating in regulating immune response and inflammatory response. Firstly, we explored the effects of TC6-D3 peptide on the migration of immune cells. As shown that the ratio of total DCs and $CCR7^+$ DCs subset in $CD45^+$ lymphocytes has no significant change whether in tumor (Fig. 7A, B), popliteal LNs (Fig. 7C), and inguinal LNs (Fig. 7D) compared to the negative control. Furthermore, by examining the proportion of $CCR7^+CD8^+$ and $CCR7^+CD4^+$ T cells, we found that TC6-D3 peptide did not affect the infiltration of $CCR7^+$ T cells in tumor tissue (Figure S7A) and popliteal LNs (Figure S7B) with only a slightly decrease in inguinal LNs (Figure S7C). Here, we also conducted the toxicity analysis. The ALT, AST, BUN, and CREA levels in serum are within institutional normal range (Figure S8). Histopathology analysis illustrated no abnormalities in major organs by hematoxylin and eosin (H&E) staining of tissue sections after treatment (Figure S9). Collectively, these results showed that the anti-tumor effect of TC6-D3 was mainly to inhibit tumor cells LN metastasis and restored anti-tumor activity of $CD8^+$ T cells without obvious immune-related side effects.

Discussion

Lymph node involvement represents a harbinger of distant metastatic disease and therefore an important prognostic factor, which enabling the suppression of antitumor immunity and ultimately generating metastasis-promoting tumor-specific immune tolerance [4]. Growing studies have indicated that highly expressed CCR7 facilitated the LN metastasis of acute lymphoblastic leukemia [32]. Moreover, overexpressed CCR7 plays a critical role in the tumor progression and LN metastasis across various solid tumors, including breast cancer, melanoma, etc. [13]. Here, we found the CCR7 expression was significantly positively correlated with LN metastasis in patients. In particularity, the specifically upregulated CCR7 was observed in secondary tumor lymph node metastasis tissue compared with distal metastasis, local metastasis, and primary melanoma by analyzing the GEO and TCGA databases.

CCR7-mediated LN metastasis plays an active role in shaping distant metastasis for various solid malignancies. Nathan E. Reticker-Flynn et al. developed a LN-specific metastasis mouse model of melanoma through an in vivo selection approach to investigate how tumors spread to LNs and whether LN colonization influences metastasis to distant tissues. The results showed that tumor cells colonizing in LN, conferred the proliferation of T regulatory cells, resisted the T cell-mediated cytotoxicity and induced immune tolerance that subsequently facilitated distant tumor

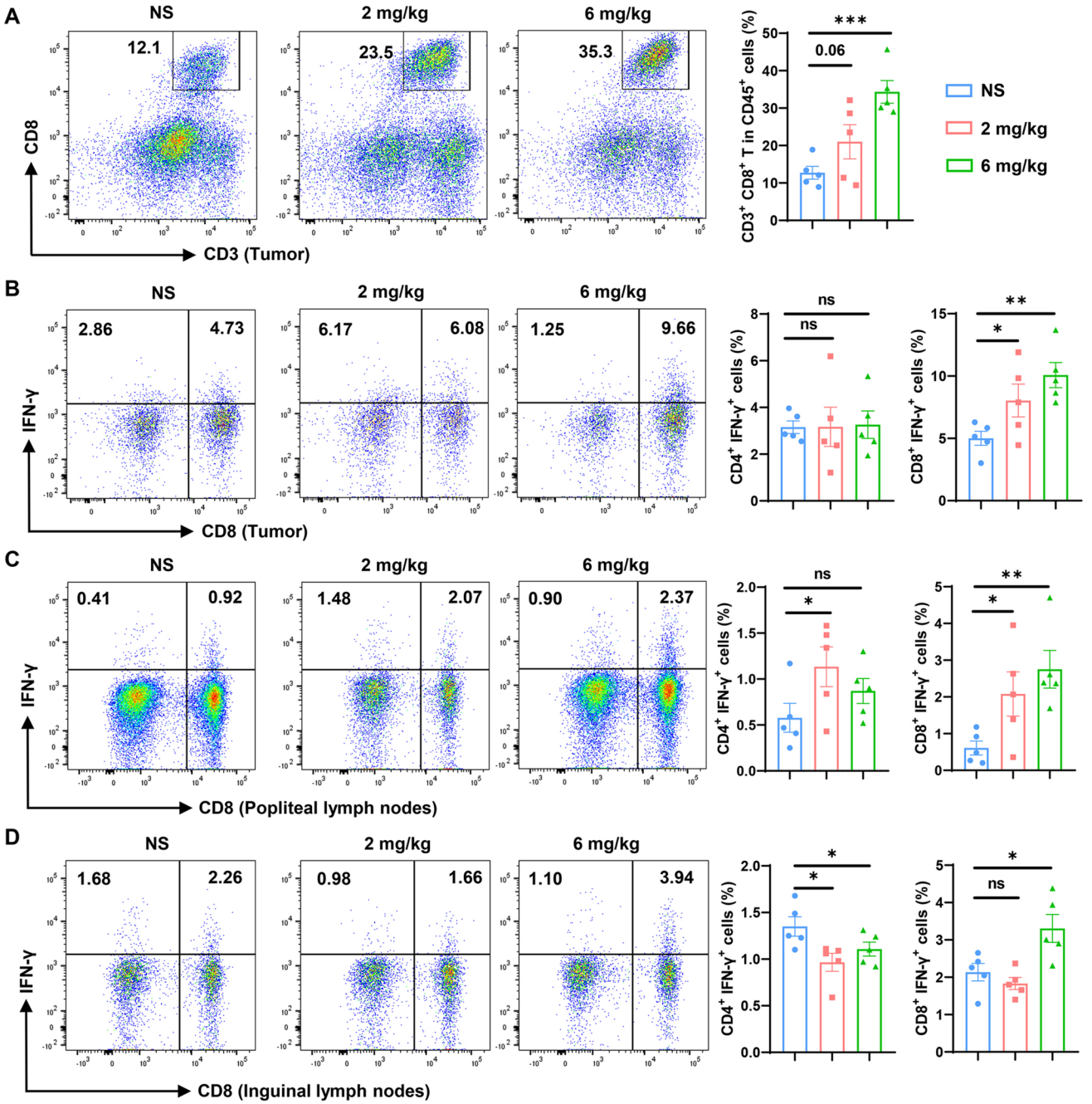

Fig. 6 TC6-D3 restored T cell-mediated anti-tumor immunity. **A** The frequencies of intratumoral $CD8^+$ T cells in $CD45^+$ lymphocytes were analyzed by flow cytometry ($n=5$). **B** Cells from tumors were stimulated with 20 ng/mL PMA and 1 μM ionomycin containing 1 μM protein transport inhibitor for 4 h. IFN-γ-secreting $CD8^+$ T cells ($CD45^+CD3^+CD8^+$) and $CD4^+$ T cells ($CD45^+CD3^+CD8^-$) were analyzed (n = 5). **C**, **D** IFN-γ-secreting $CD8^+$ T cells ($CD3^+CD8^+$ T cells) and $CD4^+$ T cells ($CD3^+CD8^-$ T cells) in popliteal lymph nodes (C) and inguinal lymph nodes (D) were analyzed by flow cytometry ($n=5$). Data are represented as means ± SEM. Student's *t* test, $^*P<0.05$, $^{**}P<0.01$, $^{***}P<0.001$, ns, not significant

colonization [4]. Next, we found the LN metastasis cell lines exhibited higher CCR7 expression than parental B16-F0 cell lines by analyzing the GSE117529 dataset, indicating that CCR7 significantly enhances the capacity of tumors to colonize in LN. Further, we demonstrated that overexpressed CCR7 in tumor cells significantly promoted LN metastasis in MC38 and B16 tumor mice models. LNs are sites of immune stimulation and surveillance, also the common sites of cancer spread and metastasis from tumor-infiltrated tissue. In LNs, tumor cells escape the killing of NK and $CD8^+$ T

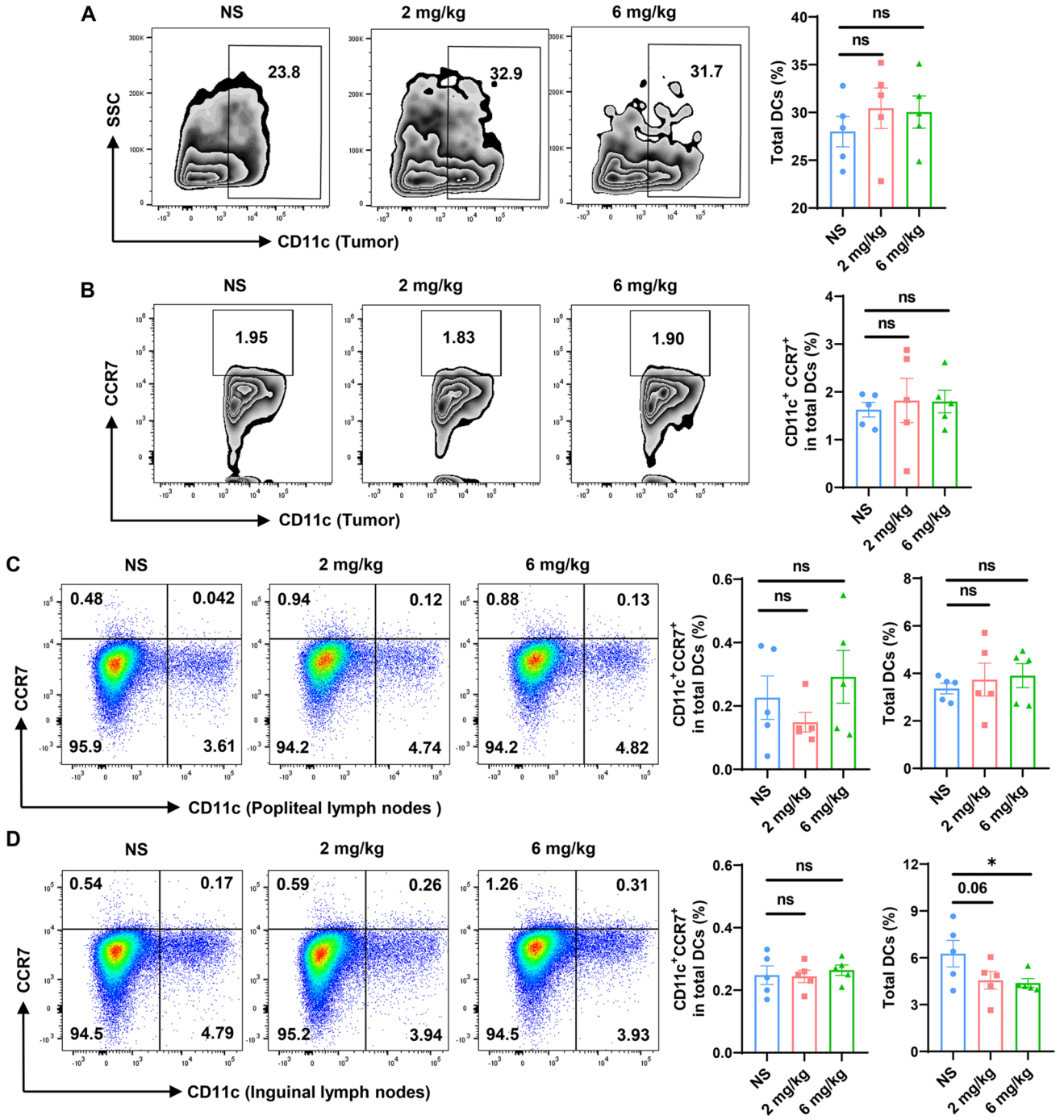

Fig. 7 TC6-D3 has no obvious effects on CCR7$^+$ immunocytes. The frequencies of total DCs (CD45$^+$CD11b$^-$CD11c$^+$) and CCR7$^+$ DCs (CD45$^+$CD11b$^-$CD11c$^+$CCR7$^+$) subsets in tumors (**A, B**), popliteal lymph nodes (**C**), and inguinal lymph nodes (**D**) were detected by flow cytometer ($n=5$). The data are presented as mean ± SEM, and the statistical significance was determined by unpaired Student's *t* test, $^*P<0.05$, ns, not significant

cells by upregulating MHC-I and PD-L1 [4, 33], as well as we observed CD8$^+$ T cells infiltrated in LN metastasis tend toward an exhausted phenotype with prominently increased expression of negative immune checkpoints such as PD-L1, PD-1, LAG-3, and TIM-3 by gene expression profiling. All these implicated tumor cells were inclined to establish an immunosuppressive microenvironment and tumor-specific immune tolerance with diversified strategies after metastasis to LNs, which further subsequently facilitated distant tumor colonization. Accordingly, blocking the CCR7 axis

can effectively inhibit the LNs metastasis and reduce the LNs burden as well as to rescue the dysfunctional T cells. This represents the potential therapeutic strategies to protract the survival of patients.

Numerous researches have indicated that the anti-CCR7 mAbs significantly delayed the tumor growth and migration to distant lymphoid organs and increased the apoptotic tumor cells in the tumor model, in addition, which drastically increased the survival of the mice in the intravenous models. In clinical trial, CAP-100, a novel therapeutic antibody-targeted human CCR7, will be evaluated in relapsed/refractory CLL patients (NCT04704323) [20, 34]. However, the antibodies poorly infiltrated into the solid tumor and induced the potent Fc-mediated complement-dependent cytotoxicity and antibody-dependent cell-mediated cytotoxicity in vivo, leading to serious treatment-related adverse events [35, 36]. Apart from antibodies, small molecule inhibitor Cmp2105 has been developed as CCR7-targeting drugs, which bind to a patch of conserved residues in the intracellular Gi protein between transmembrane helix 7 and helix 8 regions [18], but their therapeutic effects in vitro and in vivo remain unclear. Accordingly, developing inhibitors that intervene the CCR7 axis is important for therapeutic intervention against cancer.

Peptides exert a potent anti-tumor activity and might represent an interesting therapeutic alternative to conventional therapies. In this study, we identified the peptide TC6, specifically blocked CCR7/CCL19 and CCR7/CCL21 interaction by the phage display technique, and the residues L1, S2, and T12 of TC6-D3 peptide were identified as pivotal sites binding to CCR7 through the alanine scanning and computer molecular docking. Considering the weak hydrolysis stability of TC6 peptide composed with L-amino acids, we substituted it with D-amino acids from both N-terminal and C-terminal to extend its half-life and enhance the resistance to hydrolysis and named TC6-D3 peptide, which specifically affined to CCR7-GFP but not GFP with K_D values of 403 nM. Therefore, we hypothesized that TC6-D3 peptide occupies the key site of CCR7 and prevents the binding of CCR7 to CCL19 or CCL21.

In the present study, CCR7/CCL19 or CCR7/CCL21 interaction promotes cellular migration and invasion via modulation of the ERK1/2 signaling pathway and correlates with lymphatic metastasis [31, 37, 38]. Here, Western blot analysis revealed that the phospho-ERK1/2 level was markedly increased when MC38-CCR7 (GFP) or B16-CCR7 tumor cells were treated with chemokines CCL19 or CCL21, and significantly decreased when the TC6-D3 peptide was added. Correspondingly, CCL19 induced the migration of MC38-CCR7 (GFP) tumor cells in vitro, but TC6-D3 peptide depressed the effects of CCL19. Based on these results, we concluded that the activation of the CCR7/CCL19 and CCR7/CCL21 chemotaxis promoted the migration and invasion of MC38 cells and B16 cells via the ERK1/2 signaling pathway. Besides, TC6-D3 peptide significantly suppressed the ERK1/2 signaling and abrogated the effects of CCL19/CCL21 on cells migration by blocking the interaction between CCR7 and CCL19/CCL21.

Cancer cells can upregulate CCR7 expression and enable them to migrate along the gradient of CCL19 and CCL21 in lymphatic vessels and toward the LNs [39, 40]. Given the abundant lymphatic vessels in the tissue of mouse footpads, we developed a model of LN metastasis that enabled tumor cells from footpad to popliteal lymph nodes [41], as predicted CCR7 dramatically facilitated the metastasis and colonization of B16 and MC38 cells. Additionally, we showed that the treatment with TC6-D3 peptide significantly retained tumor growth and increased the infiltration of $CD8^+$ T cells in tumor and popliteal lymph nodes, as well as significantly reduced the number of CCR7-GFP^+ tumor cells that migrated from primary tumors to distant popliteal lymph nodes. In general, our results supported that TC6-D3 peptide immunotherapy might be an option for the treatment of LN metastasis.

Considering that CCR7 is expressed in major DCs and T cells, and plays an important role in stimulating dendritic cells maturation, homing, and trafficking T cells [42, 43], immune-related side effects on DC recruitment and T cell infiltration were examined when interfering in the CCR7 pathway by antibodies or genetic intervention. However, the TC6-D3 therapy group did not show significant immunosuppressive effects on DCs and T cells tracking and $CCR7^+$ DCs and $CCR7^+$ T cells infiltrating into tumor and LNs. Furthermore, the safety profile was extensively evaluated by H&E staining of the major organs and blood tests for serum biochemical markers. The peptide therapy group did not show significant differences compared with the normal saline group. These could potentially be attributed to the CCR7-targeting peptides with high affinity, relatively short circulatory half-life, and the absence of Fc-mediated ADCC and CDC effects compared with antibodies.

Although TC6-D3 has the ability to prevent tumor metastasis, there still has some limitations warranted further research, such as the expression of CCR7 on immune cells. Thus, the effect of TC6-D3 peptide on immune cell function remains to be fully elucidated. Future research should primarily develop the delivery systems that selectively binding to tumor expressed CCR7 and inhibit lymph node metastasis by blocking the CCL21/CCR7 pathway, but not the immune cells and its anti-tumor immune responses. Besides, the binding mode between TC6-D3 and CCR7 needs to be validated through protein crystallization to provide clearer structural information.

Conclusion

In summary, Tumor cells expressed CCR7 enables them metastasis to adjacent LNs to suppress the cytotoxicity of effector T cells. We screened and developed TC6-D3 peptide targeting CCR7 by phage display biopanning and substitution with D-amino acid, which specifically interfered the interaction of CCR7/CCL19 and CCR7/CCL21, and inhibited the migration of tumor cells. TC6-D3 treatment significantly delayed tumor progression, as evidenced by reduced tumor growth and enhanced the anti-tumor efficacy of T cells.

Supplementary Information The online version contains supplementary material available at https://doi.org/10.1007/s00262-025-03995-4.

Acknowledgements This work was supported by the grants from the Fundamental Research Funds for the Central Universities, Sun Yat-sen University (24qnpy187 and 24xkjc021), Shenzhen Science and Technology Program (KQTD20190929173853397), the "Pearl River Talent Plan" Innovation and Entrepreneurship Team Project of Guangdong Province (2019ZT08Y464), and the Guangdong Basic and Applied Basic Research Foundation (2022B1515120085). We are grateful to Professor XM Yang for the generous gift of B16-CCR7 cell line.

Author contributions Y.S. and Y.Q. performed the experiments, analyzed data, and prepared the paper; Y.G. and W.Z. designed the experiments, analyzed data, prepared, and revised the paper; L.Q., X.Z., H.M., L.P., X.N., Y.L., X.Z., and G.C. assisted with performing the experiments, analyzed data, and revised the paper. All authors reviewed the paper.

Funding The work was supported by the projects of the Fundamental Research Funds for the Central Universities, Sun Yat-sen University (24qnpy187 and 24xkjc021), Shenzhen Science and Technology Program (KQTD20190929173853397), the "Pearl River Talent Plan" Innovation and Entrepreneurship Team Project of Guangdong Province (2019ZT08Y464), and the Guangdong Basic and Applied Basic Research Foundation (2022B1515120085).

Data availability No datasets were generated or analyzed during the current study.

Declarations

Conflict of interest The authors declare no competing interests.

References

1. Li Y, Byun AJ, Choe JK et al (2023) Micropapillary and solid histologic patterns in N1 and N2 lymph node metastases are independent factors of poor prognosis in patients with stages II to III lung adenocarcinoma. J Thorac Oncol 18:608–619. https://doi.org/10.1016/j.jtho.2023.01.002
2. Al-Sukhni E, Attwood K, Gabriel EM, LeVea CM, Kanehira K, Nurkin SJ (2017) Lymphovascular and perineural invasion are associated with poor prognostic features and outcomes in colorectal cancer: a retrospective cohort study. Int J Surg 37:42–49. https://doi.org/10.1016/j.ijsu.2016.08.528
3. Riedel A, Shorthouse D, Haas L, Hall BA, Shields J (2016) Tumor-induced stromal reprogramming drives lymph node transformation. Nat Immunol 17:1118–1127. https://doi.org/10.1038/ni.3492
4. Reticker-Flynn NE, Zhang W, Belk JA et al (2022) Lymph node colonization induces tumor-immune tolerance to promote distant metastasis. Cell 185:1924–42.e23. https://doi.org/10.1016/j.cell.2022.04.019
5. Ubellacker JM, Tasdogan A, Ramesh V et al (2020) Lymph protects metastasizing melanoma cells from ferroptosis. Nature 585:113–118. https://doi.org/10.1038/s41586-020-2623-z
6. Su Y, Zhao B, Zhou L, Zhang Z, Shen Y, Lv H, AlQudsy LHH, Shang P (2020) Ferroptosis, a novel pharmacological mechanism of anti-cancer drugs. Cancer Lett 483:127–136. https://doi.org/10.1016/j.canlet.2020.02.015
7. Bhat AA, Nisar S, Singh M et al (2022) Cytokine- and chemokine-induced inflammatory colorectal tumor microenvironment: Emerging avenue for targeted therapy. Cancer Commun (Lond) 42:689–715. https://doi.org/10.1002/cac2.12295
8. Schumann K, Lämmermann T, Bruckner M et al (2010) Immobilized chemokine fields and soluble chemokine gradients cooperatively shape migration patterns of dendritic cells. Immunity 32:703–713. https://doi.org/10.1016/j.immuni.2010.04.017
9. Cristiani CM, Turdo A, Ventura V et al (2019) Accumulation of circulating CCR7(+) natural killer cells marks melanoma evolution and reveals a CCL19-dependent metastatic pathway. Cancer Immunol Res 7:841–852. https://doi.org/10.1158/2326-6066.Cir-18-0651
10. Jiao X, Shu G, Liu H et al (2019) The diagnostic value of chemokine/chemokine receptor pairs in hepatocellular carcinoma and colorectal liver metastasis. J Histochem Cytochem 67:299–308. https://doi.org/10.1369/0022155418824274
11. Tutunea-Fatan E, Majumder M, Xin X, Lala PK (2015) The role of CCL21/CCR7 chemokine axis in breast cancer-induced lymphangiogenesis. Mol Cancer 14:35. https://doi.org/10.1186/s12943-015-0306-4
12. Shi M, Chen D, Yang D, Liu XY (2015) CCL21-CCR7 promotes the lymph node metastasis of esophageal squamous cell carcinoma by up-regulating MUC1. J Exp Clin Cancer Res 34:149. https://doi.org/10.1186/s13046-015-0268-9
13. Salem A, Alotaibi M, Mroueh R, Basheer HA, Afarinkia K (2021) CCR7 as a therapeutic target in Cancer. Biochim Biophys Acta Rev Cancer 1875:188499. https://doi.org/10.1016/j.bbcan.2020.188499
14. Zhang L, Zhu L, Yao X et al (2022) Paclitaxel treatment enhances lymphatic metastasis of B16F10 melanoma cells via CCL21/CCR7 axis. Int J Biol Sci 18:1476–1490. https://doi.org/10.7150/ijbs.67138
15. Wu J, Li L, Liu J et al (2018) CC chemokine receptor 7 promotes triple-negative breast cancer growth and metastasis. Acta Biochim Biophys Sin (Shanghai) 50:835–842. https://doi.org/10.1093/abbs/gmy077

16. Wilson JL, Burchell J, Grimshaw MJ (2006) Endothelins induce CCR7 expression by breast tumor cells via endothelin receptor A and hypoxia-inducible factor-1. Cancer Res 66:11802–11807. https://doi.org/10.1158/0008-5472.Can-06-1222
17. Yu S, Duan J, Zhou Z, Pang Q, Wuyang J, Liu T, He X, Xinfa L, Chen Y (2008) A critical role of CCR7 in invasiveness and metastasis of SW620 colon cancer cell in vitro and in vivo. Cancer Biol Ther 7:1037–1043. https://doi.org/10.4161/cbt.7.7.6065
18. Jaeger K, Bruenle S, Weinert T et al (2019) Structural basis for allosteric ligand recognition in the human CC chemokine receptor 7. Cell 178:1222–30.e10. https://doi.org/10.1016/j.cell.2019.07.028
19. An S, Tiruthani K, Wang Y et al (2019) Locally trapping the C-C chemokine receptor type 7 by gene delivery nanoparticle inhibits lymphatic metastasis prior to tumor resection. Small 15:e1805182. https://doi.org/10.1002/smll.201805182
20. Cuesta-Mateos C, Juárez-Sánchez R, Mateu-Albero T, Loscertales J, Mol W, Terrón F, Muñoz-Calleja C (2021) Targeting cancer homing into the lymph node with a novel anti-CCR7 therapeutic antibody: the paradigm of CLL. MAbs 13:1917484. https://doi.org/10.1080/19420862.2021.1917484
21. Jiao L, Dong Q, Zhai W, Zhao W, Shi P, Wu Y, Zhou X, Gao Y (2022) A PD-L1 and VEGFR2 dual targeted peptide and its combination with irradiation for cancer immunotherapy. Pharmacol Res 182:106343. https://doi.org/10.1016/j.phrs.2022.106343
22. Zhou X, Zuo C, Li W et al (2020) A novel d-peptide identified by mirror-image phage display blocks TIGIT/PVR for cancer immunotherapy. Angew Chem Int Ed Engl 59:15114–15118. https://doi.org/10.1002/anie.202002783
23. Wang H, Sun Y, Zhou X et al (2020) CD47/SIRPα blocking peptide identification and synergistic effect with irradiation for cancer immunotherapy. J Immunother Cancer. https://doi.org/10.1136/jitc-2020-000905
24. Bellmann-Sickert K, Beck-Sickinger AG (2010) Peptide drugs to target G protein-coupled receptors. Trends Pharmacol Sci 31:434–441. https://doi.org/10.1016/j.tips.2010.06.003
25. Bockorny B, Semenisty V, Macarulla T et al (2020) BL-8040, a CXCR4 antagonist, in combination with pembrolizumab and chemotherapy for pancreatic cancer: the COMBAT trial. Nat Med 26:878–885. https://doi.org/10.1038/s41591-020-0880-x
26. Borthakur G, Ofran Y, Tallman MS et al (2021) BL-8040 CXCR4 antagonist is safe and demonstrates antileukemic activity in combination with cytarabine for the treatment of relapsed/refractory acute myelogenous leukemia: an open-label safety and efficacy phase 2a study. Cancer 127:1246–1259. https://doi.org/10.1002/cncr.33338
27. Choueiri TK, Atkins MB, Rose TL et al (2021) A phase 1b trial of the CXCR4 inhibitor mavorixafor and nivolumab in advanced renal cell carcinoma patients with no prior response to nivolumab monotherapy. Invest New Drugs 39:1019–1027. https://doi.org/10.1007/s10637-020-01058-2
28. Qian Y, Sun Y, Shi P et al (2024) Development of LAG-3/FGL1 blocking peptide and combination with radiotherapy for cancer immunotherapy. Acta Pharm Sin B 14:1150–1165. https://doi.org/10.1016/j.apsb.2023.12.011
29. Zheng H, Chen C, Luo Y et al (2021) Tumor-derived exosomal BCYRN1 activates WNT5A/VEGF-C/VEGFR3 feedforward loop to drive lymphatic metastasis of bladder cancer. Clin Transl Med 11:e497. https://doi.org/10.1002/ctm2.497
30. Askew D, Pareek TK, Eid S, Ganguly S, Tyler M, Huang AY, Letterio JJ, Cooke KR (2017) Cyclin-dependent kinase 5 activity is required for allogeneic T-cell responses after hematopoietic cell transplantation in mice. Blood 129:246–256. https://doi.org/10.1182/blood-2016-05-702738
31. Xiong Y, Huang F, Li X, Chen Z, Feng D, Jiang H, Chen W, Zhang X (2017) CCL21/CCR7 interaction promotes cellular migration and invasion via modulation of the MEK/ERK1/2 signaling pathway and correlates with lymphatic metastatic spread and poor prognosis in urinary bladder cancer. Int J Oncol 51:75–90. https://doi.org/10.3892/ijo.2017.4003
32. Buonamici S, Trimarchi T, Ruocco MG et al (2009) CCR7 signalling as an essential regulator of CNS infiltration in T-cell leukaemia. Nature 459:1000–1004. https://doi.org/10.1038/nature08020
33. Chan HL, Zhang XH (2022) Node foretold: cancer cells in lymph node rewire the immune system to enable further metastases. Cancer Cell 40:812–814. https://doi.org/10.1016/j.ccell.2022.07.001
34. Mateu-Albero T, Juárez-Sánchez R, Loscertales J, Mol W, Terrón F, Muñoz-Calleja C, Cuesta-Mateos C (2022) Effect of ibrutinib on CCR7 expression and functionality in chronic lymphocytic leukemia and its implication for the activity of CAP-100, a novel therapeutic anti-CCR7 antibody. Cancer Immunol Immunother 71:627–636. https://doi.org/10.1007/s00262-021-03014-2
35. Somovilla-Crespo B, Alfonso-Pérez M, Cuesta-Mateos C et al (2013) Anti-CCR7 therapy exerts a potent anti-tumor activity in a xenograft model of human mantle cell lymphoma. J Hematol Oncol 6:89. https://doi.org/10.1186/1756-8722-6-89
36. Cuesta-Mateos C, Fuentes P, Schrader A et al (2020) CCR7 as a novel therapeutic target in t-cell PROLYMPHOCYTIC leukemia. Biomark Res 8:54. https://doi.org/10.1186/s40364-020-00234-z
37. Shannon LA, McBurney TM, Wells MA, Roth ME, Calloway PA, Bill CA, Islam S, Vines CM (2012) CCR7/CCL19 controls expression of EDG-1 in T cells. J Biol Chem 287:11656–11664. https://doi.org/10.1074/jbc.M111.310045
38. Kohout TA, Nicholas SL, Perry SJ, Reinhart G, Junger S, Struthers RS (2004) Differential desensitization, receptor phosphorylation, beta-arrestin recruitment, and ERK1/2 activation by the two endogenous ligands for the CC chemokine receptor 7. J Biol Chem 279:23214–23222. https://doi.org/10.1074/jbc.M402125200
39. Förster R, Davalos-Misslitz AC, Rot A (2008) CCR7 and its ligands: balancing immunity and tolerance. Nat Rev Immunol 8:362–371. https://doi.org/10.1038/nri2297
40. Clatworthy MR, Aronin CE, Mathews RJ, Morgan NY, Smith KG, Germain RN (2014) Immune complexes stimulate CCR7-dependent dendritic cell migration to lymph nodes. Nat Med 20:1458–1463. https://doi.org/10.1038/nm.3709
41. Lee CK, Jeong SH, Jang C, Bae H, Kim YH, Park I, Kim SK, Koh GY (2019) Tumor metastasis to lymph nodes requires YAP-dependent metabolic adaptation. Science 363:644–649. https://doi.org/10.1126/science.aav0173
42. Alraies Z, Rivera CA, Delgado MG et al (2024) Cell shape sensing licenses dendritic cells for homeostatic migration to lymph nodes. Nat Immunol 25:1193–1206. https://doi.org/10.1038/s41590-024-01856-3
43. Liu J, Zhang X, Cheng Y, Cao X (2021) Dendritic cell migration in inflammation and immunity. Cell Mol Immunol 18:2461–2471. https://doi.org/10.1038/s41423-021-00726-4